

## **Attenuating Artificial Dissipation in the Computation of Navier–Stokes Turbulent Boundary Layers**

**E. Shalman,<sup>1</sup> A. Yakhot,<sup>1</sup> S. Shalman,<sup>1</sup> O. Igra,<sup>1</sup> and Y. Yadlin<sup>2</sup>**

*Received March 26, 1996*

---

We propose a new formulation of the fourth-difference artificial dissipation coefficient needed for the Navier–Stokes solutions. This coefficient is scaled by a damping function which is expressed in terms of the Baldwin–Lomax algebraic turbulence model. The suggested scaling function damps the artificial dissipation across the boundary layer. The objective of this paper is to test the ability of the suggested damped scaling coefficient to provide (a) a given accuracy on a coarser grid; and (b) an accurate computing of turbulent boundary layers. To accomplish this, attached and separated transonic flows over the NACA 0012 airfoil, and turbulent flow over a flat plate have been considered.

---

**KEY WORDS:** Artificial dissipation; fourth-difference coefficient; airfoil flows.

### **1. INTRODUCTION**

Various approaches based on the concept of artificial dissipation were originally developed for the Euler methods of computing inviscid flows in order to control numerical instabilities and to allow the capture of shock waves. The Euler equations do not have a physical dissipation mechanism and the artificial dissipation damps oscillations in the solution. Recently, there has been a strong trend toward using the Navier–Stokes formulation of viscous transonic flows, even though it can be computationally expensive. The Navier–Stokes equations contain natural viscous dissipation effects which are significant in thin viscous shear layers, but are insignificant in the inviscid region of the flow. In practice, the artificial dissipation

---

<sup>1</sup> Pearlstone Center for Aeronautical Engineering Studies, Department of Mechanical Engineering, Ben-Gurion University of the Negev, Beersheva 84105, Israel.

<sup>2</sup> McDonnell Douglas Aerospace, Advanced Transport Aircraft Development, Mail stop 71-35, 2401 E. Wardlow Rd., Long Beach, California 90807-4418.

is still needed for the Navier–Stokes computations since the physical dissipation, inherent in the viscous terms, is insufficient to stabilize the scheme in the regions outside the shear layer.

Jameson *et al.* (1981) first proposed an artificial dissipation model which incorporates a linear combination of second- and fourth-difference dissipation terms. The scaling coefficients are scalar and isotropic. It is clear that for thin viscous shear layers, where the second and higher velocity derivatives are naturally large, an artificial dissipation will contaminate the computing of the boundary layer stresses and the skin friction. Moreover, in this model the artificial dissipation term is proportional to the grid spacing, and only for fine-grid computations may one expect high-accuracy resolution of boundary layers. On the other hand, using fine grids inevitably leads to additional computational efforts.

The challenging problem is to derive a form of artificial dissipation that does not affect the accuracy of viscous shear layer computations but contributes to the numerical convergence by smoothing the rest of the numerical solution. During the last ten years considerable progress has been made to achieve this goal, and attempts have been devised to define a scalar or a matrix dissipation coefficient. The matrix coefficient proposed by Turkel (1988) separately scales the dissipation associated with each dependent variable. For a given grid, this matrix dissipation requires more computational efforts than the scalar dissipation. Recently reported calculations [Swanson and Turkel (1992); Turkel and Vatsa (1994)] show that a given accuracy can be achieved on a coarser grid, so that the computer time is effectively less than that required to obtain the same accuracy with scalar dissipation. Hall (1994) introduced a reducing factor for artificial dissipation that is based on the magnitude of the physical (viscous) dissipation and is of vector form. Comparing the results, Hall (1994) concludes that for some cases his vector dissipation method matches in accuracy the matrix dissipation method of Swanson and Turkel (1992), and a relatively high accuracy can be achieved on coarse grids. With regard to the scalar dissipation, we note Martinelli's work (1987) where the scaling coefficient is modified by including a function of the spectral radii of the inviscid flux Jacobian matrices.

Reddy and Papadakis (1993) performed computations with dissipation added only to the inviscid part of the flow while dissipation in the boundary layer was turned off. They left open the question about the selection of "boundary layer grid points" in Navier–Stokes solutions. For some cases, the results obtained with this simple stepwise model agree fairly well with the results of the boundary layer code.

In this paper we propose a different approach to the fourth-difference dissipation coefficient. This coefficient, still scalar, is scaled by a damping

function which is expressed in terms of a turbulence model used in Navier–Stokes solutions. It is commonly accepted that the artificial dissipation should be scaled (damped) within a shear layer, and we suggest a turbulent length scale as a measure of this layer. For computing transonic turbulent flows over an airfoil, the Baldwin–Lomax algebraic turbulence model (BLM) is widely used. We introduce a new scaling coefficient based on the vorticity function employed by the BLM to define a turbulent length scale. The objective of this paper is to test the ability of the suggested damped scaling coefficient to provide (a) a given accuracy on a coarser grid; and (b) an accurate computing of turbulent boundary layers. To accomplish this, attached and separated transonic flows over the NACA 0012 airfoil, and turbulent flow over a flat plate have been considered. It would be misleading to evaluate the accuracy of a numerical solution only on the basis of force (pressure and lift) coefficients. Acceptable pressure distributions and lift coefficients can be obtained without accurately modeling the properties in the boundary layer. In the present study, the emphasis has been on the effects of grid refinement on lift, drag and skin friction, and on comparison of the computed velocity distributions with the classic turbulent boundary layer velocity profiles.

## 2. NUMERICAL SCHEME

We use the Multigrid Diagonal Implicit (MDI) algorithm of Caughey (1988), extended to solve the Thin-Layer Navier–Stokes equations, which are appropriate for high Reynolds number flows [Varma and Caughey (1991)]. The equations are discretized using finite volumes with cell averaged quantities used for the dependent variables. In order to prevent odd-even point decoupling and oscillations near shock waves and stagnation points, an artificial dissipation is added as an adaptive blend of second- and fourth-order differences. The difference approximation of the governing equations, including the dissipative terms, can be written

$$\frac{dw_{i,j}}{dt} + Qw_{i,j} - Dw_{i,j} = 0 \quad (2.1)$$

where  $w$  is the solution vector of conservative variables,  $Q$  is an operator representing the differences introduced by approximations for the fluxes, and  $D$  is an operator representing the dissipative terms. The dissipative operator is defined by

$$Dw = D_{\xi}w + D_{\eta}w \quad (2.2)$$

where

$$D_\xi w = d_\xi(d_\xi w), \quad D_\eta w = \delta_\eta(d_\eta w) \quad (2.3)$$

Here  $\delta_\xi$  and  $\delta_\eta$  are central-difference operators and

$$d_\xi = \varepsilon^{(2)} \delta_\xi - \varepsilon^{(4)} \delta_\xi^3, \quad d_\eta = \varepsilon^{(2)} \delta_\eta - \varepsilon^{(4)} \delta_\eta^3 \quad (2.4)$$

The coefficients of dissipation, following Caughey (1988), are defined as follows. Let the ratio of pressure gradient to total pressure ( $\gamma$ ) for the cell ( $i, j$ ) be given by

$$\gamma_{i,j} = \frac{|p_{i+1,j} - 2p_{i,j} + p_{i-1,j}|}{|p_{i+1,j} + 2p_{i,j} + p_{i-1,j}|} \quad (2.5)$$

Then

$$\varepsilon_{i+1/2,j}^{(2)} = k^{(2)} \max(\gamma_{i+1,j}, \gamma_{i,j}) \quad (2.6)$$

and

$$\varepsilon_{i+1/2,j}^{(4)} = \max[0, k^{(4)}/64 - \varepsilon_{i+1/2,j}^{(2)}] \quad (2.7)$$

where  $k^{(2)}$  and  $k^{(4)}$  are the second- and fourth-order dissipation coefficients. The function  $\gamma$  is a limiter (i.e., switching) function, in the sense that it activates the second- or fourth-difference dissipation contribution based on the pressure gradient, and is discussed later.

To construct an iterative scheme, the equations, including the artificial dissipation terms, are written in differential form. The spatial derivatives are approximated implicitly, and the change in the flux vectors are linearized in time. The implicit operator thus obtained is approximated as a product of two (three in 3D) one-dimensional factors. For numerical efficiency, these factors are diagonalized using local similarity transformations. Since it is not possible to diagonalize simultaneously the Euler and the viscous fluxes, the latter are kept purely explicit. This results in a set of 4 (5 in 3D) scalar pentadiagonal systems for each grid point. The error introduced in the factorization is  $O(\Delta t^2)$  and in the diagonalization is of  $O(\Delta t)$ . The convergence of the solution of the difference equations to steady state is accelerated using local time-stepping and multigrid. In local time stepping, the maximum possible time step in each individual cell is used. This destroys the time accuracy of the solution but does not affect the steady-state solution. The multigrid technique accelerates convergence by eliminating the low wave number errors, treating them as high wave numbers on the coarse grids. Boundary conditions are imposed numerically

using a single layer of dummy cells. Values for the dependent variables at these cells are assigned using explicit boundary conditions. Due to the implicit character of the scheme, implicit boundary conditions are imposed on the solution variables before the solution of the system of equations. A complete description of the numerical algorithm can be found in Caughey (1988); Yadlin and Caughey (1990); and Varma and Caughey (1991).

### 3. ALGEBRAIC TURBULENCE MODELS

In the next sections we introduce a new formulation of the fourth-difference coefficient  $k^{(4)}$  based on parameters of the Baldwin–Lomax algebraic turbulence model [Baldwin and Lomax (1978)]. We also consider flow problems to verify the new  $k^{(4)}$  formulation using the Baldwin–Lomax and the algebraic- $Q_4$  turbulence model recently developed by us [Yakhot *et al.* (1996)]. In this section we provide a short description of these algebraic models.

#### 3.1. Baldwin–Lomax Model (BLM)

The most popular turbulence models, the eddy viscosity models, which have been widely used in engineering computations, are based on a two-layer concept wherein the boundary layer is formally split into inner and outer regions. Different turbulent length and velocity scales are used in these regions. In the two-layer Baldwin–Lomax model [Baldwin and Lomax (1978)], the turbulent viscosity is defined differently in the inner and outer regions. In the inner region, the classical Prandtl mixing length formulation is used, viz.

$$v_{\text{inner}} = l_{\text{inner}}^2 \Omega, \quad l_{\text{inner}} = \kappa y D \quad (3.1)$$

where the vorticity  $\Omega$  is defined by  $\Omega = (2\Omega_{ij}^2)^{1/2}$ ,  $\Omega_{ij} = \frac{1}{2}(\partial U_i/\partial x_j - \partial U_j/\partial x_i)$ ,  $\kappa$  is the von Karman constant and  $D$  is the van Driest damping function.

The Baldwin–Lomax algebraic eddy viscosity model has been developed for separated turbulent flows. To define the turbulent length scale in the outer region, the BLM employs the vorticity function  $F = y\Omega D$ . The eddy viscosity in the outer region is defined by

$$v_{\text{outer}} = \alpha C_1 F_{BL} F_{KLEB} \quad (3.2)$$

where  $\alpha = 0.0168$ ,  $C_1 = 1.6$ ,  $F_{Kleb}$  is Klebanoff's intermittency function, and  $F_{BL}$  is defined by

$$F_{BL} = \min(y_{\text{max}} F_{\text{max}}, y_{\text{max}} U_{\text{diff}}^2 / 4F_{\text{max}}) \quad (3.3)$$

Here  $F_{\max}$  is the maximum value of the vorticity function  $F$  that occurs in the velocity profile and  $y_{\max}$  is the normal to the wall  $y$ -location where  $F$  takes the maximum value.  $U_{\text{diff}}$  is the difference between maximum and minimum velocity in the velocity profile.

For attached boundary layer flows, the BLM is based on the quantities  $F_{\max}$  and  $y_{\max}$  which could be interpreted as a characteristic velocity and length, respectively, and are determined from the function  $F = y\Omega D$ . For separated flows, turbulent characteristic length and velocity are associated with  $y_{\max}$  and  $U_{\text{diff}}^2/F_{\max}$ , respectively.

### 3.2. Algebraic- $Q_4$ Model

An algebraic eddy viscosity model, based on a new length scale, has recently been developed by Yakhot *et al.* (1996). The model proposes the total (molecular plus turbulent) viscosity  $\nu$  as a solution of a quartic ( $Q_4$ ) equation, viz.

$$Q_4(\nu) = \nu^4 + (C - 1) \nu_0^3 \nu - (\kappa^2 \Omega l^2)^4 = 0, \quad \nu = \max(\nu, \nu_0) \quad (3.4)$$

where  $C \approx 2000$  is a constant. An important feature of Eq. (3.4) is that the turbulent viscosity turns on (in the sense that  $\nu > \nu_0$ ) when

$$\kappa^2 \Omega l^2 \nu_0^{-1} > C^{1/4} \quad (3.5)$$

In other words, the algebraic- $Q_4$  equation implies the existence of a viscous sublayer where the non-dimensional number  $\kappa^2 \Omega l^2 \nu_0^{-1}$ , which is in fact a local Reynolds number, is less than the threshold  $C^{1/4}$ . For the case of a fully turbulent regime when  $\nu \gg \nu_0$ ,  $\nu \approx \nu_{\text{turb}}$ , one can neglect the second term in Eq. (3.4). In this case, we obtain from Eq. (3.4)  $\nu_{\text{turb}} \approx \kappa^2 \Omega l^2$ , which is the classic Prandtl mixing-length formulation.

Like other algebraic turbulence models, the  $Q_4$ -model requires a definition for the turbulent length scale. To define the length scale in the outer region the vorticity function  $F = y\Omega D$ , introduced in the BLM, is used. The length scale  $l$  appearing in Eq. (3.4) is defined as

$$l = \min(y, \gamma y_{\max}) \quad (3.6)$$

From (3.6), the length scale in the inner region is defined as  $l_{\text{inner}} = y$ . The length scale in the outer region is  $l_{\text{outer}} = \gamma y_{\max}$ , where  $\gamma$  is the intermittency coefficient which should be different for different types of flows. Based on analytical considerations and numerical computations of attached,

separated and wake flows, the value of the intermittency coefficient  $\gamma$  is specified as

$$\gamma = \begin{cases} 0.25 & \text{if } U_{\max}/F_{\max} < 2.0 \\ 0.45 & \text{if } U_{\max}/F_{\max} > 2.0 \end{cases} \quad (3.7)$$

where  $U_{\max}$  is the velocity at the location where the vorticity function  $F$  takes the maximum value  $F_{\max}$ .

Finally, the algebraic- $Q_4$  turbulence model of Yakhot *et al.* (1996) is defined by Eqs. (3.4), (3.6), and (3.7).

#### 4. FOURTH-DIFFERENCE DISSIPATION COEFFICIENT, $k^{(4)}$

Examination of the expressions for  $\varepsilon^{(2)}$  and  $\varepsilon^{(4)}$  shows that in regions of flow discontinuities pressure gradients are large, thus  $\gamma_{i,j}$  is large and the second-order term  $\varepsilon^{(2)}$  is dominant. In regions of smooth flow  $\gamma_{i,j}$  is very small, hence  $\varepsilon^{(2)}$  is negligible and  $\varepsilon^{(4)}$  is emphasized. The fourth-difference coefficient  $k^{(4)}$  controls the magnitude of the fourth-order artificial dissipation term  $\varepsilon^{(4)}$ . This means that the computation of a smooth flow (boundary layer) can be contaminated by a poor choice (too large) of  $k^{(4)}$ . The typical values of the dissipation coefficients  $k^{(2)}$  and  $k^{(4)}$  for multigrid schemes are  $1/2 \div 2$  and  $1 \div 2$ , respectively. The values generally used in the MDI algorithm are  $k^{(2)} = 2$  and  $k^{(4)} = 2$  [Caughey (1988)]. In the present calculations, we use  $k^{(2)} = 2$ , while the choice of the fourth-difference coefficient  $k^{(4)}$  is the subject of the study.

Following the analysis of the difference stencils for the scalar dissipation in the vicinity of the boundaries, performed by Swanson and Turkel (1993) for the case of laminar viscous flows, we have for turbulent boundary layers

$$D_{\eta} \propto k^{(4)} \phi \Delta \bar{\eta} Re^{\alpha} \quad (4.1)$$

where  $\phi$  is the aspect ratio,  $\Delta \bar{\eta}$  is the grid spacing across the boundary layer, and  $Re$  is the Reynolds number. From Eq. (4.1), it is seen that to keep the artificial dissipation small the resolution increases for the high- $Re$  boundary layers. As it follows from Eq. (4.1), one should expect poor accuracy for the boundary layer calculation when coarse or high aspect ratio meshes are used, unless the value of  $k^{(4)}$  is extremely small. On the other hand, such a *globally* small value of  $k^{(4)}$  will have a severe adverse effect on the convergence rate of a multigrid scheme. Reddy and Papadakis (1993) performed computations with dissipation added *only* to the inviscid part of the flow while dissipation in the boundary layer was turned off.

They use a “no dissipation in the boundary layer” model in which the dissipation is set to zero at a fixed number of grid rows normal to the wall. The authors left open the question of the selection of “boundary layer grid points” in Navier–Stokes solutions. However, for some cases, the results obtained with this simple stepwise model agree fairly well with the results of the boundary layer code. For complex flows with separation, determining the “no dissipation boundary layer” can lead to serious numerical difficulties.

In this paper we propose a different approach to the fourth-difference dissipation coefficient  $k^{(4)}$ . It is commonly accepted that the artificial dissipation should be scaled (damped) within the shear layer, and we suggest a turbulent length scale as a measure of this layer. In computing transonic turbulent flows over an airfoil, the Baldwin–Lomax algebraic turbulence model (BLM) is widely used. To introduce a new scaling coefficient, we use the vorticity function  $F = y\Omega D$  employed by the BLM. In the BLM, a turbulent length scale is defined in terms of the distance  $y_{\max}$  (measured normal to the wall  $y$ -direction), where  $F$  takes the maximum value  $F_{\max}$ . It seems plausible to suppose that  $y_{\max}$  provides a simple measure of the viscous flow region. To attenuate the artificial dissipation in the regions where viscous effects are dominant, we suggest scaling the fourth-difference coefficient  $k^{(4)}$  by a damping function

$$f(y) = \left( \frac{y}{y + y_{\max}} \right)^2 \quad (4.2)$$

It can be shown that for attached boundary layers [Stock and Haase (1987)]  $y_{\max} \approx 0.5 \delta$ , and, therefore, at the edge of the boundary layer  $f(\delta) = 4/9$  while  $f(\delta/2) = 1/4$ . The suggested scaling function  $f(y)$  damps the artificial dissipation across the boundary layer, and the fourth-difference coefficient is, hereafter, called the damped  $k^{(4)}$ . In the case of Thin Layer Navier–Stokes Approximation, the artificial dissipation ( $D$ ) should be damped only in the direction across the boundary layer:  $D = D_\xi + f(\eta) D_\eta$ .

## 5. NUMERICAL RESULTS

In this section we present the results of computations of three flow problems to show the influence of the fourth-difference dissipation coefficient,  $k^{(4)}$ , on the accuracy of turbulent boundary layer calculations. Computations were performed for attached and separated flows around the NACA 0012 airfoil, and for turbulent flow over a flat plate. We used  $k^{(4)} = 1.0$  multiplied by the scaling factor in Eq. (4.2) which is, hereafter, called the damped  $k^{(4)}$ .

The finest computational mesh for the airfoil computations consists of  $640 \times 128$  mesh points, and of  $1280 \times 128$  for flow over a flat plate with 62.5% of the points fitted on the airfoil. Special attention has been paid in order to resolve a boundary layer; enough mesh points having been placed in the vicinity of the wall. The error has been estimated as the logarithm of the residual (the average of  $|\Delta\rho/\Delta t|$  over all cells in the grid). For all computations, the residual is reduced nearly six-seven orders of magnitude on the finest mesh of the multigrid cycle, and consistent convergence for all cycles has been achieved.

We employed two turbulence models: the Baldwin-Lomax model, and the algebraic- $Q_4$  recently developed by us [Yakhot *et al.* (1996)]. Performances of both models for all numerically simulated cases are compared.

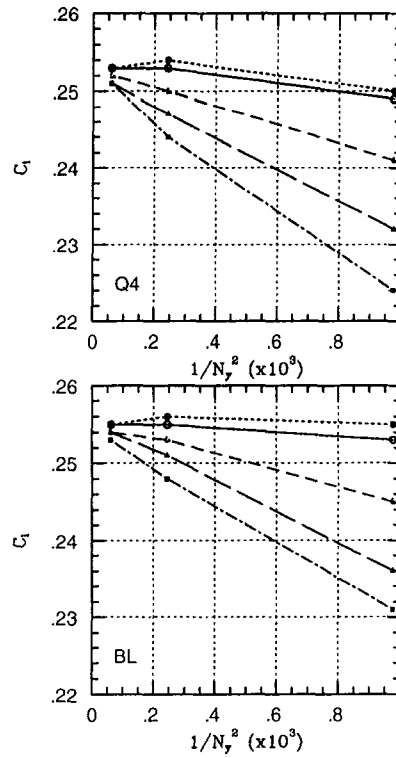


Fig. 1. Lift coefficient  $C_l$  for different grids. NACA 0012 airfoil,  $M_\infty = 0.7$ ,  $\alpha^\circ = 1.49$ ,  $Re_c = 9.0 \cdot 10^6$ . Solid: damped  $k^{(4)}$ ; short dash:  $k^{(4)} = 0.1$ ; dash:  $k^{(4)} = 0.5$ ; long dash:  $k^{(4)} = 1.0$ ; dash-dot-dash:  $k^{(4)} = 2.0$ .

### 5.1. Attached Airfoil Flow

For this problem, we use the NACA 0012 airfoil. The free-stream Mach number,  $M_\infty$ , is 0.7, the angle of attack,  $\alpha'$ , is  $1.49^\circ$ , and the Reynolds number based on the airfoil chord,  $Re_c$ , is  $9.0 \cdot 10^6$ . In this case, the flow is attached and just slightly supersonic near the airfoil leading-edge [Holst (1988)]. At  $x/c \approx 0.15$  a very weak shock wave occurred and is followed by the recovery region where an attached boundary layer is developed.

In Figs. 1–3 we present the lift ( $C_l$ ), drag ( $C_d$ ) and friction ( $C_f$ ) coefficients obtained with the standard and damped fourth-difference dissipation coefficients  $k^{(4)}$ . It should be noted that the lift  $C_l$  is less affected by the artificial dissipation than the drag  $C_d$ . The latter directly depends on the accuracy of calculation of the skin friction which can be contaminated by the poor choice of the  $k^{(4)}$ .

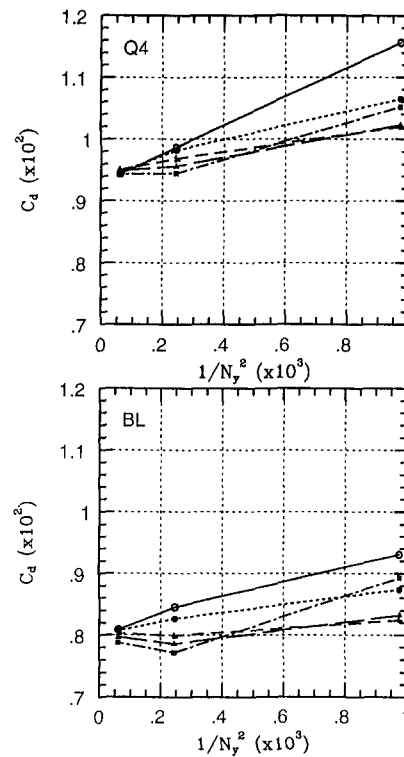


Fig. 2. Drag coefficient  $C_d$  for different grids. For legend see Fig. 1.

In Fig. 1, the lift coefficients ( $C_l$ ), computed with two different turbulence models for three successive computation meshes ( $160 \times 32$ ,  $320 \times 64$ , and  $640 \times 128$ ), are presented. The close-to-constant behavior of the damped  $k^{(4)}$  curve boldly illustrates that the results converge even on a coarse-grid. There is only a slight departure from the results obtained with the smallest standard  $k^{(4)} = 0.1$  which could be considered as nearly free of artificial dissipation contamination. We recall that, in general, the values of the standard  $k^{(4)}$  less than 0.5 should be considered as undesirable for the Navier–Stokes solutions of complex transonic flows due to convergence restrictions. Comparing the data for the standard  $k^{(4)} = 1.0$  and 2.0 with the damped  $k^{(4)}$  results evidently shows that the suggested damped  $k^{(4)}$  accelerates convergence considerably. From Fig. 1, there is almost no qualitative or quantitative difference between the lift coefficients ( $C_l$ ) computed with the BL or  $Q_4$  algebraic turbulence models.

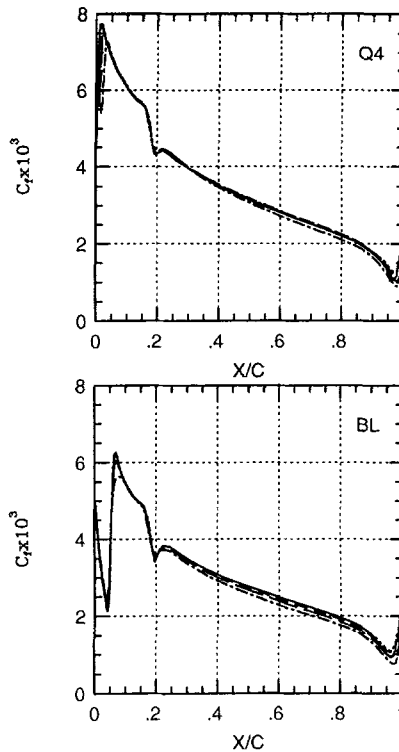


Fig. 3. Friction coefficient  $C_f$ , upper surface,  $640 \times 128$  grid. For legend see Fig. 1.

In Fig. 2, the drag coefficients ( $C_d$ ), computed with two different turbulence models for three successive computation meshes ( $160 \times 32$ ,  $320 \times 64$ , and  $640 \times 128$ ), are shown. It is seen that on the finest grid of  $640 \times 128$  the results are nearly unaffected by the  $k^{(4)}$ . The effect of the  $k^{(4)}$  shows up on the  $320 \times 64$  grid. One can see that the  $320 \times 64$  grid results obtained with the algebraic- $Q_4$  model are less sensitive to the choice of  $k^{(4)}$  than ones obtained with the Baldwin-Lomax (BL) model.

The distributions of the skin friction coefficient ( $C_f$ ), computed on the upper-surface of the airfoil with two different turbulence models, are shown Fig. 3 for the finest  $640 \times 128$  grid, and in Fig. 4 for the  $320 \times 64$  grid. In Figs. 3 and 4 one can distinguish four flow regimes: laminar, transitional to turbulent, very weak shock wave, and recovery region where an attached boundary layer is developed. From Fig. 3, as was noted earlier for the drag coefficient, the distributions of the skin friction computed on the finest grid of  $640 \times 128$  are nearly unaffected by the  $k^{(4)}$  (especially when the

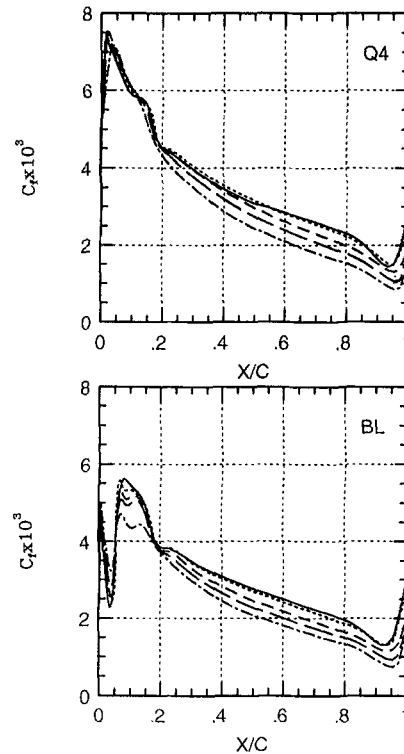


Fig. 4. Friction coefficient  $C_f$ , upper surface,  $320 \times 64$  grid. For legend see Fig. 1.

algebraic- $Q_4$  turbulence model was used). In Fig. 4, we present the distributions of the skin friction computed on the  $320 \times 64$  grid where the influence of the  $k^{(4)}$  shows up. One can see that the dependency on the  $k^{(4)}$  is similar for both turbulence models within the attached boundary layer region ( $x/c > 0.2$ ). On the other hand, within transitional to turbulence and up to the shock wave location narrow region ( $0.1 < x/c < 0.2$ ), only the  $C_f$  curves computed with the BL model are affected by the choice of the  $k^{(4)}$ . From Figs. 3 and 4, it should be emphasized that the damped  $k^{(4)}$  curves differ only slightly from the results obtained with the smallest standard  $k^{(4)} = 0.1$  which could be considered as nearly free of artificial dissipation contamination. Moreover, the results obtained with the damped  $k^{(4)}$  on the coarse  $320 \times 64$  grid are very similar to the ones obtained on the finest  $640 \times 128$  grid. On the other hand, it is seen that the results obtained on the two successive meshes with the standard  $k^{(4)} = 1.0$  are considerably different, which could be considered as the lack of grid refinement convergence.

Using the principle of Richardson extrapolation, one can estimate a numerical error under the assumption that the results on the two finest grids are of second-order accuracy and can be extrapolated to the exact (in the sense of infinitesimally small grid) solution,  $C_l^{(0)}$  and  $C_D^{(0)}$ . In this way, the results in Figs. 1 and 2, yielding the percentage errors in lift and drag,  $\Delta C_l$  and  $\Delta C_d$ , are summarized in Table I.

A correct prediction of the universal logarithmic velocity law is an important test for the ability of a numerical scheme with an artificial

**Table I.** NACA 0012,  $M_\infty = 0.7$ ,  $\alpha^\circ = 1.49^\circ$ : Summary of Errors in Lift  $C_l$  and Drag  $C_D$

$k^{(4)}$	Grid	Baldwin-Lomax model		Algebraic- $Q_4$ model	
		$\Delta C_l/C_l^{(0)}$	$\Delta C_D/C_D^{(0)}$	$\Delta C_l/C_l^{(0)}$	$\Delta C_D/C_D^{(0)}$
2.0	$160 \times 32$	0.093	0.126	0.116	0.116
	$320 \times 64$	0.026	0.027	0.037	0.002
	$640 \times 128$	0.007	0.007	0.009	0.000
1.0	$160 \times 32$	0.075	0.041	0.081	0.080
	$320 \times 64$	0.016	0.018	0.021	0.010
	$640 \times 128$	0.004	0.004	0.005	0.003
0.1	$160 \times 32$	0.001	0.091	0.011	0.138
	$320 \times 64$	0.005	0.032	0.005	0.049
	$640 \times 128$	0.001	0.008	0.001	0.012
damped	$160 \times 32$	0.008	0.168	0.016	0.244
	$320 \times 64$	0.000	0.061	0.000	0.060
	$640 \times 128$	0.000	0.015	0.000	0.015

dissipation to resolve the turbulent boundary layer with a high-order of accuracy. In Figs. 5–7, we show the mean velocity distributions expressed in wall units. The profiles are computed with different fourth-difference dissipation coefficients,  $k^{(4)}$ , for two successive computation meshes (dashed line:  $320 \times 64$ , and solid line:  $640 \times 128$ ). From Figs. 5–7, for the finest grid, one can clearly see a pronounced logarithmic velocity profile which is an indication of the sufficient resolution of the turbulent boundary layer. The distributions (for both turbulence models) obtained on the finest  $640 \times 128$  grid are close enough to conclude that these results are nearly unaffected by the fourth-order artificial dissipation coefficient  $k^{(4)}$ . There is a certain difference between the universal log-law shift constant predicted by two turbulence models, however its discussion is outside the scope of this paper. Consistent with the discussion of the skin friction distributions, the velocity profile obtained with the damped  $k^{(4)}$  on the coarse  $320 \times 64$  grid (Fig. 5,

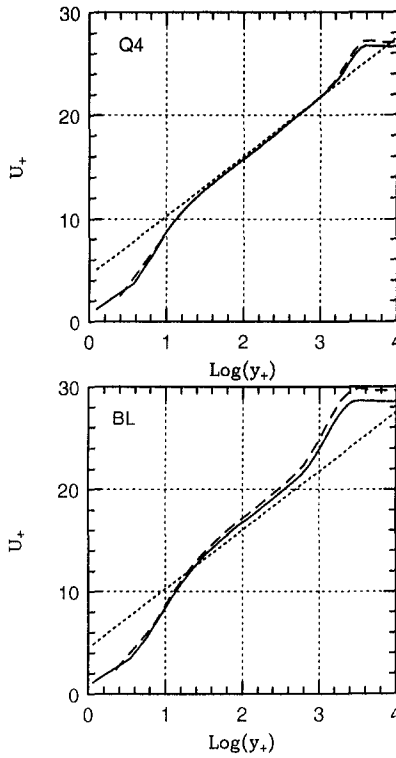


**Fig. 5.** Mean velocity profile measured in wall units, damped  $k^{(4)}$ . NACA 0012 airfoil,  $M_\infty = 0.7$ ,  $\alpha^\circ = 1.49$ ,  $Re_c = 9.0 \cdot 10^6$ , upper surface,  $X/C = 0.5$ . Solid line:  $640 \times 128$  mesh; dashed line:  $320 \times 64$ ; short-dashed line:  $U_+ = 2.5 \text{Log}(y_+) + 4.5$ .

dashed line) is very similar to the one obtained (especially with the algebraic- $Q_4$  turbulence model) on the finest  $640 \times 128$  grid (Fig. 5, solid line). On the other hand, it is seen that the results obtained on the two successive meshes with the standard  $k^{(4)} = 1.0$  and  $2.0$  (Figs. 6 and 7) are considerably different. This confirms that the fourth-difference standard coefficients  $k^{(4)} = 1.0$  or  $2.0$ , while having positive effect on the convergence rate of multigrid scheme, have a severely contaminating effect on the computation of near-wall turbulent viscous flows.

## 5.2. Separated Airfoil Flow

For this problem, we use the NACA 0012 airfoil. The free-stream Mach number,  $M_\infty$ , is 0.799, the angle of attack,  $\alpha^\circ$ , is  $2.26^\circ$ , and the Reynolds number based on the airfoil chord,  $Re_c$ , is  $9.0 \cdot 10^6$ . In this case, a shock wave exists on the airfoil upper surface at  $x/c \approx 0.5$ . This shock wave is

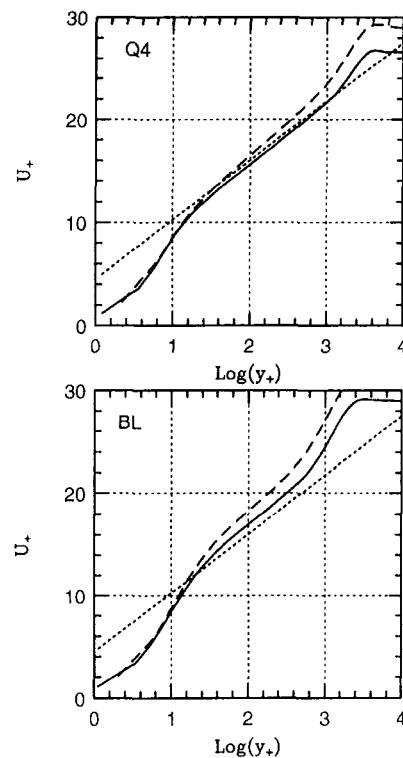


Fig. 6. Mean velocity profile measured in wall units,  $k^{(4)} = 1.0$ . For legend see Fig. 5.

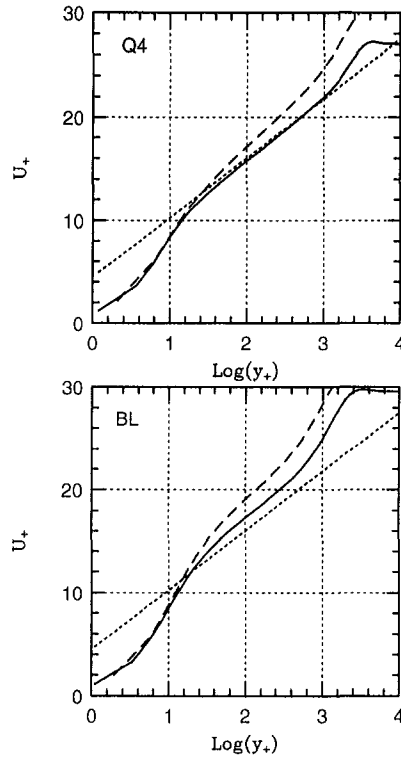


Fig. 7. Mean velocity profile measured in wall units,  $k^{(4)} = 2.0$ . For legend see Fig. 5.

strong enough to cause significant boundary layer separation. For this case, no special clustering of mesh points near the shock has been used. The emphasis has been on the effects of grid refinement on lift and drag, while the capture of the shock location and steepness have been ignored. In Figs. 8 and 9, the values of lift ( $C_l$ ) and drag ( $C_d$ ), computed for three successive computation meshes ( $160 \times 32$ ,  $320 \times 64$ , and  $640 \times 128$ ), are presented. These results are obtained for two different turbulence models with the standard and damped scaling dissipation coefficients  $k^{(4)}$ . The significant deviation of the results computed with the standard  $k^{(4)} = 1.0$  (dashed line) from the straight line deserves some comments. The assumption is that the numerical scheme employed is of second-order accuracy and one can expect that, for sufficiently fine grids (small  $N_y^{-2}$ ), computed results should lie on a straight line. This is not the case when the results obtained with the standard  $k^{(4)} = 1.0$  on a coarse  $160 \times 32$  grid where, apparently, higher than the second-order difference terms contaminate the numerical

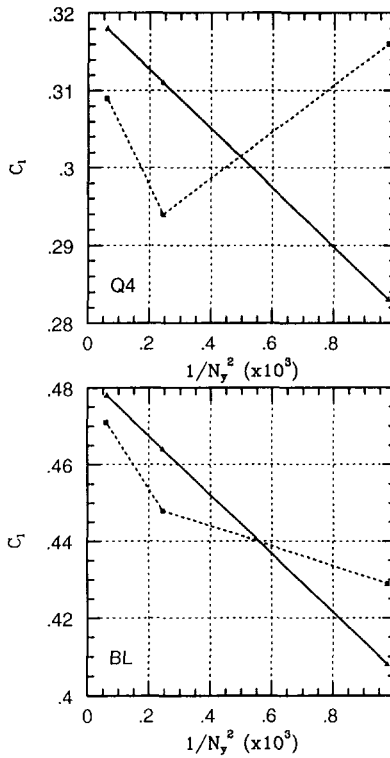


Fig. 8. Lift coefficient  $C_l$  for different grids. NACA 0012 airfoil,  $M_\infty = 0.799$ ,  $\alpha^\circ = 2.26$ ,  $Re_c = 9.0 \cdot 10^6$ . Solid: damped  $k^{(4)}$ ; short dash:  $k^{(4)} = 0.1$ ; dash:  $k^{(4)} = 0.5$ ; long dash:  $k^{(4)} = 1.0$ ; dash-dot-dash:  $k^{(4)} = 2.0$ .

solution. On the other hand, the results obtained with the damped  $k^{(4)} = 1.0$  for three successive computation meshes lie on a straight line (solid line).

### 5.3. Flat-Plate Flow

To test the ability of the suggested damped scaling coefficient to provide an accurate computation of turbulent boundary layers we consider flow over a flat plate. For this problem, we use a very thick airfoil with the geometry set up as follows: a semi-ellipse leading edge (1% chord), constant 0.4% thickness from 1% to 95% chord, and a wedge trailing edge. The free-stream Mach number  $M_\infty$  is 0.5, the Reynolds number based on the chord length is  $9 \cdot 10^6$ , and the angle of attack is zero. To avoid instabilities originating at the leading edge due to the small separation bubble, the

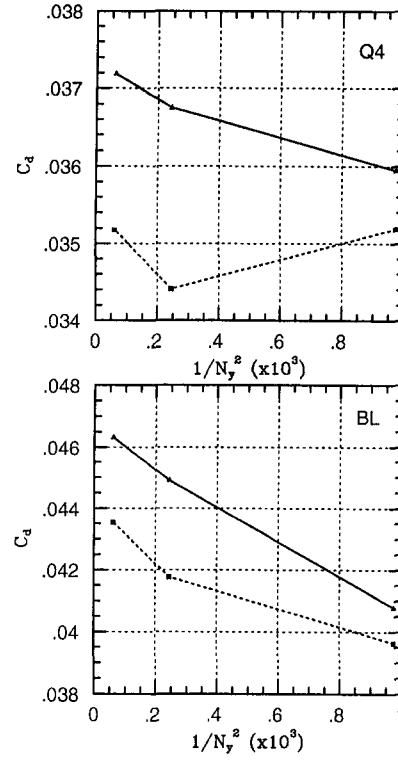


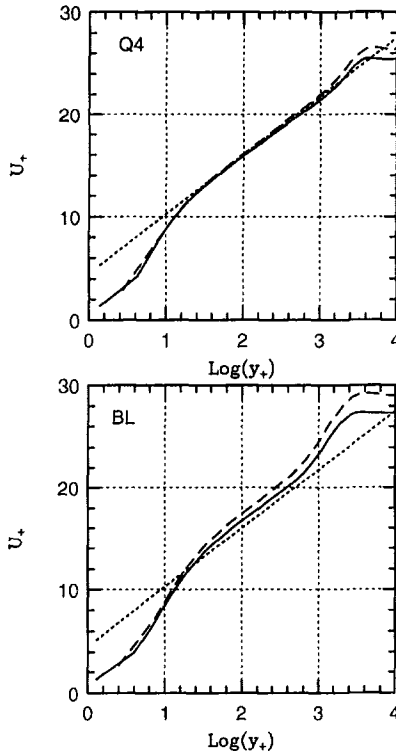
Fig. 9. Drag coefficient  $C_D$  for different grids. For legend see Fig. 8.

Table II. Flat Plate: Summary of Errors in Friction Coefficient  $C_f$ ,  $Re_L = 9 \cdot 10^6$ ,  $x/L = 0.5$

$k^{(4)}$	Grid	Baldwin-Lomax model		Algebraic- $Q_4$ model	
		$C_f (\times 10^3)$	$\Delta C_f / C_f^{(0)}$	$C_f (\times 10^3)$	$\Delta C_f / C_f^{(0)}$
2.0	$320 \times 32$	1.047	0.577	1.169	0.615
	$640 \times 64$	1.737	0.299	1.993	0.344
	$1280 \times 128$	2.291	0.075	2.776	0.086
1.0	$320 \times 32$	1.084	0.561	1.456	0.508
	$320 \times 64$	1.949	0.211	2.326	0.214
	$1280 \times 128$	2.340	0.053	2.800	0.053
0.1	$320 \times 32$	2.109	0.142	2.552	0.125
	$640 \times 64$	2.484	0.073	2.998	0.016
	$1280 \times 128$	2.631	0.018	3.035	0.004
damped	$320 \times 32$	2.201	0.173	2.742	0.083
	$640 \times 64$	2.496	0.062	3.010	0.006
	$1280 \times 128$	2.620	0.016	2.995	0.002

laminar-turbulence transition was fixed at 1.2% plate (chord) length. The computations were performed using the C-grid. The results for three successive computation meshes ( $320 \times 32$ ,  $640 \times 64$ , and  $1280 \times 128$ ) of the multigrid cycle are presented. For high-accuracy resolutions 62.5% of the grid points were fitted on the plate.

The calculated values of the skin-friction coefficient  $C_f$  at  $Re_x = 4.5 \cdot 10^6$  are listed in Table II. We note that the skin-friction coefficient computed with the explicit correlation formula  $C_f = 0.455/\ln^2(0.06 Re_x)$  [White (1974)] is  $2.91 \cdot 10^{-3}$ . Comparison of the  $C_f$  distribution along the plate with different correlation formulas is outside the scope of this paper. We estimate a numerical error under the assumption that the results on the two finest grids are of second-order accuracy and can be extrapolated to the exact (in the sense of infinitesimally small grid) solution,  $C_f^{(0)}$ . It is seen that only the results obtained with the small standard  $k^{(4)} = 0.1$  and with



**Fig. 10.** Flat-plate. Mean velocity profile measured in wall units, damped  $k^{(4)}$ .  $Re_L = 9.0 \cdot 10^6$ ,  $X/C = 0.5$ . Solid line:  $1280 \times 128$  mesh; dashed line:  $640 \times 64$ ; short-dashed line:  $U_+ = 2.5 \text{Log}(y_+) + 4.5$ .

the damped  $k^{(4)}$  could be considered as converged. Moreover, the results with the algebraic- $Q_4$  turbulence model are converged even on the  $640 \times 64$  grid. It confirms that the damped  $k^{(4)}$  reduces the contamination of the viscous flow calculation while alleviating the convergence of the numerical scheme. The results with the fourth-difference standard coefficients  $k^{(4)} = 1.0$  or  $2.0$  cannot be considered as converged even on the finest  $1280 \times 128$  grid. This means that the high value of the standard  $k^{(4)}$  has a contamination effect on the accuracy of computing the skin friction. From Table II, the results obtained with the damped  $k^{(4)}$  on the two successive finest meshes are, practically, identical to the corresponding results with the standard  $k^{(4)} = 0.1$ . We recall that, in general, the results with the small standard  $k^{(4)} = 0.1$  could be considered as nearly free of artificial dissipation contamination.

In the present study, the emphasis has been on the effects of grid refinement on skin friction, and on comparison of the computed velocity

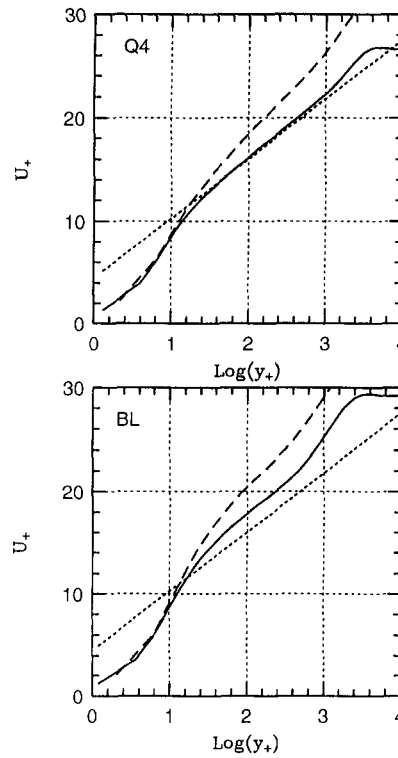


Fig. 11. Flat-plate. Mean velocity profile measured in wall units,  $k^{(4)} = 2.0$ . For legend see Fig. 10.

distributions with the classic turbulent boundary layer velocity profiles. A correct prediction of the universal logarithmic velocity law is an important test for the ability of a numerical scheme with an artificial dissipation to resolve the turbulent boundary layer with a high-order of accuracy.

In Figs. 10 and 11, we show the mean velocity distributions expressed in wall units. The profiles are computed with two successive computation meshes (dashed line:  $640 \times 64$ , and solid line:  $1280 \times 128$ ). From Fig. 10 (damped  $k^{(4)}$ ), for the  $Q_4$  turbulence model, one can clearly see a pronounced logarithmic velocity profile which is an indication of the sufficient resolution of the turbulent boundary layer. Moreover, the distributions (for both grids) are very close; thus we conclude that these results are nearly unaffected by the grid refinement. On the other hand, the logarithmic velocity profile obtained with the Baldwin–Lomax model on the relatively coarse  $640 \times 64$  grid shows (Fig. 10, dashed line) a slightly overpredicted shift:  $U_+ = 2.5 \ln(y_+) + 5.9$ . For the standard  $k^{(4)} = 2.0$ , from Fig. 11, only the results obtained with the  $Q_4$  turbulence model on the finest  $1280 \times 128$  grid could be considered as sufficiently resolved and unaffected by the artificial dissipation.

## 6. CONCLUSIONS

A new approach to the fourth-difference dissipation coefficient is proposed. This coefficient is scaled by a damping factor which is expressed in terms of the vorticity function employed by the Baldwin–Lomax turbulence model to define a turbulent length scale. Attached and separated transonic flows over the NACA 0012 airfoil, and turbulent flow over a flat plate have been considered. Numerical tests have shown that the new formulation of the damped fourth-difference dissipation coefficient  $k^{(4)}$  allows attenuating the artificial dissipation providing (a) a given accuracy on a relatively coarse grid; and (b) an accurate computation of turbulent boundary layers.

## ACKNOWLEDGMENTS

This research was supported by The Israel Science Foundation administered by The Israel Academy of Sciences and Humanities.

## REFERENCES

- Baldwin, B. S., and Lomax, H. (1972). Thin layer approximation and algebraic model for separated turbulent flows, AIAA Paper 78-257.
- Caughey, D. A. (1988). Diagonal implicit multigrid algorithm for the Euler equations, *AIAA J.* **26**, 841–851.

- Hall, M. G. (1994). On the reduction of artificial viscosity in viscous flow solutions. In Caughey, D. A., and Hafez, M. M. (eds.), *Frontiers of Computational Fluid Dynamics*, John Wiley, pp. 303–317.
- Holst, T. L. (1988). Viscous transonic airfoil workshop compendium of results, AIAA Paper 87-1640.
- Jameson, A., Schmidt, W., and Turkel, E. (1981). Numerical solutions of the Euler equations by finite volume methods using Runge–Kutta time-stepping schemes, AIAA Paper 81-1259.
- Martinelli, L. (1987). Calculations of viscous flows with multigrid methods, Ph.D. dissertation, Princeton University, MAE Department.
- Reddy, S., and Papadakis, M. (1993). Artificial viscosity models for Navier–Stokes equations and their effect in drag prediction, AIAA Paper 93-0193.
- Stock, H. W., and Haase, W. (1987). The determination of turbulent length scales in algebraic turbulence models for attached and slightly separated flows using Navier–Stokes methods, AIAA Paper 87-1302.
- Swanson, R. C., and Turkel, E. (1992). On central difference and upwind schemes, *J. Comput. Physics* **101**, 292–306.
- Swanson, R. C., and Turkel, E. (1993). Aspects of a high-resolution scheme for the Navier–Stokes equations, AIAA Paper 93-3372.
- Turkel, E. (1988). Improving the accuracy of central difference schemes, *11th Intl. Conf. Numerical Methods in Fluid Dynamics*, Springer-Verlag, New York, *Lecture Notes in Physics* **323**, 586–591.
- Turkel, E., and Vatsa, V. N. (1994). Effect of artificial viscosity on three-dimensional flow solutions, *AIAA J.* **32**, 39–45.
- Varma, R. R., and Caughey, D. A. (1991). Diagonal implicit multigrid solution of compressible turbulent flows, AIAA Paper 91-1571.
- White, F. M. (1974). *Viscous Fluid Flow*, McGraw-Hill, New York.
- Yadlin, Y., and Caughey, D. A. (1990). Block multigrid implicit solution of the Euler equations of compressible fluid flow, *AIAA J.* **29**, 712–719.
- Yakhot, A., Shalman, E., Igra, O., and Yadlin, Y. (1996). An algebraic- $Q_4$  turbulence model for transonic airfoil flows, *J. Sci. Comput.* **11**(2), 71–98.